

S-Duct Inlet Analysis and Design for Small TurboJet Applications

Orange Team: Ryan Platt, Zackary Krawczyk, Haden Glasgow, Aidan Dartlon, Braydon Revard, Nick Zizzo
Mechanical & Aerospace Engineering, Stillwater, Oklahoma, 74075

This report outlines the process of designing an S-duct inlet for a JetCat P100-RX engine that satisfies the requirements of the 2020-2021 APOP design challenge. For the inlet design three design parameters were optimized. These are: axial length, capture area, and inlet geometry. Through the use of a moment arm test stand and mass flow rate parameter, a variety of inlets were tested on the JetCat engine with the goal being to minimize performance losses by changing the design parameters. These inlets were 3-D printed using a Creatbot F430 3-D printer. A testing matrix along with computational fluid dynamic simulations in the CAD software Solidworks was used in order to pinpoint the optimum inlet design. Experimental results for pressure recovery were evaluated utilizing a static pressure ring and Kiel probes for total pressure measurement. Experimentation indicated that the primary criteria of pressure recovery was negligible and decreasing axial length proved to have negligible effects as well so the capture area could be further decreased as all engine parameters, except potentially the SFC values, meet the requirements set out by AFRL. While there is some question as to the validity of the SFC, testing has demonstrated that a short inlet with two 90 degree turns will perform acceptably while maintaining a relatively small volume. Further testing and validation may need to be performed for the final inlet design choice as experimental results were not able to be obtained within the bounds of this project.

Nomenclature

<i>AFRL</i>	=	Air Force Research Laboratory
<i>CFD</i>	=	computational fluid dynamics
c_p	=	constant pressure specific heat
F	=	uninstalled thrust
<i>FEA</i>	=	finite element analysis
f	=	fuel/air ratio
g_c	=	proportionality constant
γ	=	specific heat ratio
η	=	component efficiency
M	=	Mach Number
<i>MFP</i>	=	mass flow parameter
\dot{m}	=	mass flow rate
<i>OSHA</i>	=	Occupational Safety and Health Administration
P	=	static pressure
P_t	=	total pressure
<i>PPE</i>	=	personal protective equipment
π	=	total pressure ratio
<i>SFC</i>	=	specific fuel consumption
T_t	=	total temperature
<i>TSFC</i>	=	thrust specific fuel consumption
<i>WDM</i>	=	weighted decision matrix

I. Introduction

A. Problem Description

This paper presents the Aerospace Propulsion Outreach Program (APOP) design challenge for 2020-2021 which tasks students to develop an S-Duct inlet for the JetCat P100-RX. This inlet will allow for future engine airframe integration, as engines are typically mounted along the centerline of an airframe with a ducted inlet that extends to the capture area. For this project, the new inlet design transports flow from a single capture area that is 6 inches from the centerline of the JetCat engine. The AFLR provided Fig. 1 shows a representation of the vertical distance between the engine centerline and the inlet capture area.

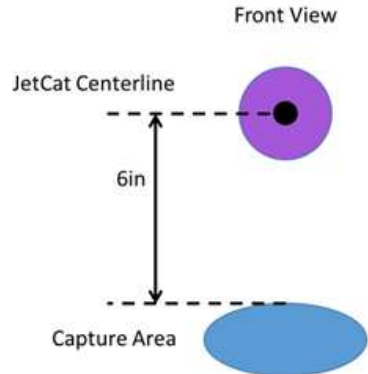


Figure 1. Inlet Offset Requirement

The main goal of this inlet design will be to minimize the performance losses of the JetCat engine. In order to achieve this, the inlet will minimize total pressure losses and distortion of the airflow entering the engine. By doing this, the maximum thrust and thrust specific fuel consumption (TSFC) will be as close as possible to reference operating conditions. These reference conditions will be measured by way of engine tests with the Air Force Research Laboratory's (AFRL) bell mouth inlet design attached to the JetCat engine. The S-duct inlet will then be attached and the engine's performance will be recorded and compared. These tests will be conducted on the AFRL test stand. An example of this process can be seen below in Fig. 2.

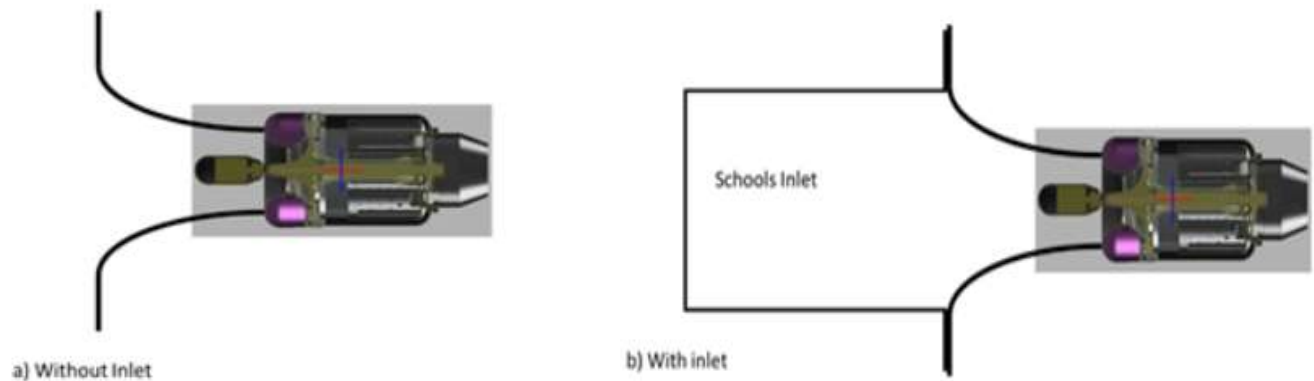


Figure 2 . Inlet Testing Method

The S-duct inlet performance goals can be broken down into primary and secondary objectives. No matter the inlet design, the primary objectives should be achieved in order for this project to be a success. The secondary criteria are additional goals that will ultimately distinguish successful inlets from each other. The primary and secondary goals criteria can be seen below:

Primary objectives

- a total pressure recovery that is greater than or equal to 98%
- a maximum thrust decrement of less than 5%
- a TSFC decrement of less than 5%

Secondary objectives

- minimization of the axial inlet length
- minimization of total inlet volume

The minimization of the inlet size is advantageous, as this allows for additional payload, fuel, or structure that will improve the mission capabilities of an airframe designed around this engine configuration.

B. Stakeholders

For this project, three major stakeholders have been identified. These include the Air Force, Oklahoma State University, and defense contractors. The Air Force is the primary stakeholder in the project, as they are the organization which directly proposed and funded the project, providing all requirements and criteria in the statement of work and will directly benefit from the findings or innovative designs which may be presented. Knowing this, their needs and priorities took precedent over all of the other stakeholders as the Air Force's impression of this project will ultimately determine the success of the project.

Oklahoma State University is the next major stakeholder in this project as all research, fabrication, and testing took place within facilities owned by the University, and any successful design and patents will be published with the University attached to it. It was important to stay in good standing with the University by abiding by all university and department policies throughout the project to ensure minimal delays and to prevent possible reprimand.

The last major stakeholder is any defense contractors which may stand to benefit from the results of this design project, as its findings may prove useful to the technological development of small UAV craft. This stakeholder drives the design modifiability for implementation onto aircraft which may need to meet specific mission requirements such as operating in multiple orientations, fitting onto an airframe without impeding other subsystems of the aircraft, and being fabricated from materials which will not be affected by varying temperature and pressure altitudes. In order to meet the needs of this stakeholder, additional relevant information was documented about the inlet. The biggest example of this is recommending an in-flight inlet design recommendation and discussing advantages of the PEEK 3-D printer material.

II. Project Safety and Management

A. Environmental Health and Safety Considerations

Some of the factors that would affect the design included the environmental, health, and safety considerations. These considerations would serve to keep all members engaged with the project safe while also affecting decisions about how to limit the social, economical, and environmental contentions. The team aimed to identify as many of these factors as possible, in order to conduct the designing and testing in a way to mitigate these into as much of a nonfactor as possible. While there is a duty to AFRL to provide the best possible product, there is also a duty to everyone affected by the project as a whole; balancing these responsibilities served as a guiding force in the design process.

Several safety procedures were lined out to ensure the safety of all members and bystanders during engine testing. Personnel were to stand a distance of no less than 5 feet away from the engine to stay clear from the exhaust gases and the extreme heat. Ear protection and eye protection were to always be used when the engine was in operation. A fire extinguisher must always be available and on standby in case of a critical device failure to limit as much damage as possible to personnel and to the equipment. Finally, the testing stand had all structural loads tested to ensure that no structural failure is possible in any foreseeable fashion.

With respect to the COVID-19 pandemic, all personnel had PPE (personal protective equipment) in use as well as following all the guidelines set in place by Oklahoma State University, such as the use of facemask when in a proximity of less than 6' distance. Proper sanitation was also used by personnel and the test stand to keep health safety as a top priority.

Finally, environmental concerns were identified that would be mitigated to keep the environment clean and minimize social impact. Project members were to only print parts that were necessary and run the engine once a week to keep it operating in peak condition but not test excessively to minimize pollutants from the fuel. The limited printing would lessen the waste and also free the printer for other APOP teams or individuals who needed time to print for their project. Aiming for smaller build volumes also helps mitigate the material use consideration. Finally, guidelines for proper fuel storage were made, starting with ensuring all fuel lines were connected properly, and that any spills are carefully cleaned up with equipment designed for such purpose.

B. Safety Guidelines

Beyond the social and environmental considerations that guided out design and shaped the processes by which the team conducted themselves and the project, professional guidelines that outline all sorts of engineering considerations and safety concerns were followed. From the National Archives and Records Administrations’ Aeronautics and Space guidelines: 14 C.F.R. § 33.75-33.78 (2021), the following sections of concern were abided by: safety analysis and engine ingestion. As it pertains to the safety analysis, careful noting of all safety guidelines governing engine mounting systems and the section on controls. For the engine ingestion concerns, careful observation of the foreign object ingestion guidelines as well as the section detailing operation in rain and hail and the safety concerns those can dictate for engine ingestion were made. The guidelines from the Occupational Safety and Health Administration (OSHA), Section 1910 were also considered. The guidelines covered encompassed PPE usage, proper sanitation, the use of a fire extinguisher, wiring design and protection, hazardous locations, and the storage of flammable liquids. Due to the scope of the project being the design and testing of a small engine, the degree to which careful adherence to safety guidelines was important but not critical. Failure on a project this small scale would be of no great cost, severe injury, or a delay of more than a couple weeks. While important, the guidelines were not something that strongly geared the impact of the design beyond the obvious safety and cost measures. With all these considerations and guidelines in place, work on designing the inlet began.

C. Risk Management

The team had to collectively consider a number of risks and created mitigation plans to decrease the severity of the consequences to an acceptable level. As can be seen below in Table 2, weighting was given to the severity of a consequence with the probability of the consequence occurring. Risks were broken down into three types: cost risks, safety risks, and schedule risks. Severity and probability values were given to each risk, leading to a priority number. Based on the given priority number, the status of either open or closed was given. Open status meant that the project can progress without needing to further address risk mitigation, and closed status meant that risk mitigation must be further implemented before the project could advance.

Table 2: Risk Management Table

		IMPACT				
		VERY LOW 0.05	LOW 0.1	MEDIUM 0.2	HIGH 0.4	VERY HIGH 0.8
PROBABILITY	VERY LIKELY 90%	0.05	0.09	0.18	0.36	0.72
	LIKELY 70%	0.04	0.07	0.14	0.28	0.56
	POSSIBLE 50%	0.03	0.05	0.10	0.20	0.4
	UNLIKELY 30%	0.02	0.03	0.06	0.12	0.24
	RARE 10%	0.01	0.01	0.02	0.04	0.04

Description	Risk Type	Impact(Severity)	Probability	Priority	Status
Unforeseen Costs, like 3D printed materials and tools	Cost	Medium	Unlikely	0.06	Open
Spread of COVID-19 causing quarantine	Safety	Medium	Possible	0.1	Open
Hearing Damage from Engine Testing	Safety	Medium	Rare	0.02	Open
Eye Damage from Engine Testing or Part Fabrication	Safety	Medium	Rare	0.02	Open
Long 3D printing times causing missed deadlines	Schedule	High	Unlikely	0.12	Open
Test Stand Part Fabrication and Shipping Delays	Schedule	Medium	Rare	0.02	Open

D. Knowledge Gaps

There were some gaps in what was known going into the start phase of testing. The first of these is how well the CFD results fit with reality. This was unknown and was tested as a part of the first phase of testing. Testing with the pressure equipment was the main way to fill in this knowledge gap. Initially, there was uncertainty over how much of the axial length could be reduced while completing the requirements assigned by AFRL. This knowledge gap was overcome by extensive CFD testing, and models from eighteen to sixteen inches all performed well enough for different shapes and face areas to be used. Model interior changes were something both teams were not sure of, since the effects of friction and guiding structures (dimples, ridges, etc) have been unknown outside of modeling. However, pressure testing using the kiel probes allows for better understanding and application for the design of inlets.

III. Background and Theory

A reliable and accurate form of measuring engine performance is critical to assessing influence of an inlet design. To do this, a moment arm thrust stand was designed to accomplish this. A representation of this test stand can be seen in Fig. 3. As seen below, the Jetcat engine was mounted toward the top of the mount away from the table in order to mitigate flow effects from the surroundings. The mount itself was constructed from aluminum T-slotted rails. This frame was then fixed to the table through the use of mounted ball bearings. This configuration allows the frame to rotate about the bearings with minimum frictional losses to measure thrust. A load cell was placed in front of the bearings on another moment arm that is rigidly attached to the engine arm in order to measure the resultant force produced when the engine is activated.

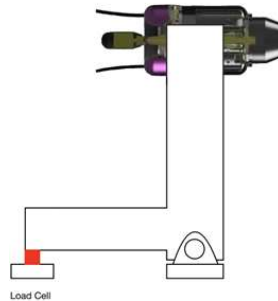


Figure 3. Test Stand Representation

This design was chosen as it is simple, efficient, quick to build, and can easily be modified to accommodate various components. This is due to the way that this configuration measures the thrust produced by the engine. An idealization of the forces present on the test stand can be seen below in Fig. 4. The “Reaction Force” will be the force seen by the load cell. By summing the moments about point A, which is the axis of rotation due to the mounted bearings, the thrust can be calculated through the use of equation 1.

$$T = \frac{R_y * L_c}{L_g} \quad (1)$$

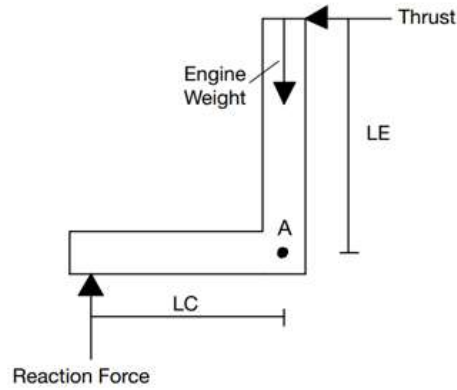


Figure 4. Test Stand Moment Forces

This equation assumes that the weight of the engine is exactly vertical from point A. Naturally, during the installation of the various inlets, the center of gravity of the engine will change, which will affect the load cell reading. These inaccuracies will be taken into account through careful calibration. To account for the difference in center of gravities, the load cell will be tarred to zero with each new inlet that is tested. This will provide accurate and reliable thrust data to compare between various inlet tests.

As it can also be seen in equation 1, by varying the lengths of the moment arms, a variety of load cells with different ratings can be utilized. This will provide a great benefit in the case that any components break or fail, simply changing the configuration will allow for a straightforward replacement process that will minimize delays.

A. Mass Flow Parameter (MFP)

Initially, it was assumed that a 4 inch diameter inlet would be an ideal starting point as that would involve the least amount of geometry change within the inlet from the capture area to the bell mouth transition piece which also had a 4 inch diameter. Using that assumption and the manufacturer's reported mass flow rate at maximum thrust of $\dot{m} = 0.5512$ lbm/sec in equation 2, outputs a mach number at various sections within the inlet. This allowed for velocity to be calculated which was used for Fanno Flow analysis and when running CFD both in static flow simulations and when testing inlets for flight conditions.

$$MFP = \frac{\dot{m}}{A} * \frac{\sqrt{T_T}}{P_T} = \sqrt{\frac{\gamma g_c}{R}} M \left(1 + \frac{\gamma-1}{2} M^2 \right)^{\frac{\gamma+1}{2(\gamma-1)}} \quad (2)$$

B. Fanno Flow

Fanno flow analysis was used to understand the effect that friction has on the performance of the designed inlet. For the fanno flow analysis, it was assumed that the curvature of the S-duct inlet contributes no additional losses for the analysis and was treated as a straight pipe. The knowns in the analysis were the Mach number at the inlet face, the ratio of specific heat of air, and an approximated friction factor of the 3D printed PEEK material that the final inlet will be printed with. With the desired percent pressure recovery of 98% known, an optimum length over diameter ratio for the inlet was determined. The L/D ratio was then utilized in the design process when choosing the capture area and axial length of the designed inlet. The Fanno flow results demonstrated the length needed to accelerate the flow from the first Mach Number to the second using boundary layer nozzle effects. This length was useful in showing the magnitude of the effects of Fanno flow, for example a very large length to diameter ratio would show that the effects of Fanno flow are fairly negligible. The key Fanno Flow equations used in calculations can be seen below.

$$\frac{4fL^*}{D} = \frac{1-M^2}{\gamma M^2} + \frac{(\gamma+1)}{2\gamma} \ln\left(\frac{(\gamma+1)M^2}{2+(\gamma-1)M^2}\right) \quad (3)$$

$$\frac{P_0}{P_0^*} = \frac{1}{M} \left(\frac{2+(\gamma-1)M^2}{(\gamma+1)}\right)^{\frac{(\gamma+1)}{2(\gamma-1)}} \quad (4)$$

Due to the various assumptions built into the Fanno flow equations, the values obtained are used for preliminary estimations as opposed to final results. This analysis was mainly used to check the pressure recovery to ensure the pressure would not dip below the ninety-eight percent minimum put in place by AFRL. Using this minimum, an optimal length to diameter ratio could be found. In addition, the current frictional effects could also be tested for the current concept. This was done by finding the average diameter and using this to find the length of straight pipe needed to accelerate the flow using boundary layer effects. The length of inlet needed to reach this second Mach Number was found to be very large, suggesting the effects to be negligible.

There are a variety of assumptions associated with Fanno flow analysis that have repercussions on the results. The flow must be one dimensional, steady state, adiabatic. In addition, the flow must be travelling through a straight duct, leading to geometric inconsistencies between the requirements of the inlet and the analysis. In addition, the Fanno flow analysis also has a friction factor assumption. Since the geometry is very different for the s-duct inlet than a straight duct, there is a chance this assumption could lead to results that are not representative of reality.

C. Corrected Parameters

In order to properly compare test parameters that were captured on different days, corrected parameters must be used. Corrected Parameters are dimensionless parameters used for extrapolation of data to a common reference point so that data can be easily compared. This removes the influence of varying atmospheric conditions on the data. The pertinent parameters to be corrected for data processing are thrust and specific fuel consumption.

$$\delta_i = \frac{P_{ti}}{P_{ref}} \quad (5)$$

$$\theta_i = \frac{T_{ti}}{T_{ref}} \quad (6)$$

$$\dot{m}_{fc} = \frac{\dot{m}_f}{\delta_2 \sqrt{\theta_2}} \quad (7)$$

$$F_c = \frac{F}{\theta_i} \quad (8)$$

$$S_c = \pi d \frac{\dot{m}_{fc}}{F_c} \quad (9)$$

D. Computational Fluid Dynamics

In order to find general trends for the various inlet design parameters, CFD analysis was utilized. It is important to note that CFD was a major factor in the design of each inlet. The analysis completed using this system was a driving factor throughout much of the process. Observations of pressure and the state of the flow were the primary functions in conducting the CFD analysis. The pressure, being an important indicator of flow quality and a scoring criteria, and although there is a two percent pressure loss buffer, it was decided that to be safe the pressure recovery shown using CFD should be above ninety-nine percent. This was a trend to be followed until further pressure testing could be done. Once the reality-theoretical difference could be found, new inlet concepts could be created, ideally consisting of models with minimal volume and axial length. The models which contain the least volume can only be attained if the pressure recovery is still well above ninety-eight percent in the experimental data. The other function of CFD is the flow distortion. Using the software, there can be more visual evidence as to how the flow is moving through the inlet. With this known, mitigation plans can be put in place to reduce separation and increase the quality of the flow. A big way to mitigate much of the separation is through surface roughness. Areas that seem to be prone to separation can be intentionally more rough than other areas in the inside of the inlet so that the flow stays attached for longer.

Another use of CFD is the ability to test different conditions quickly. While trying to test different air speeds experimentally can mean waiting for the perfect conditions, CFD allows for quick iteration using these conditions. This ease of changing the entrance conditions is useful as it allows for testing to see how well the current design works at other conditions. These could include conditions closer to those seen during flight or just a range of airspeeds and pressures that could be closer to those seen in testing locations. Predictions such as these are useful in that, even though they are not perfectly representative of reality, trends still exist and can be used to create an inlet that meets the design objectives.

The concept of flight conditions was discussed as each team worked on an altered version of their current designs that is adjusted for flight conditions. CFD was heavily used as these concepts will not be able to be truly tested without the use of a wind tunnel. The model tweaked for flight conditions is presented as a CAD model with the CFD data but was not printed. Mainly, this inlet concept was solely for the purpose of showing a slightly better model for actual flight. The reason for this design exploration is that the mass flow parameter analysis was completed only to design for a static test. Designing an inlet for simulated flight conditions is not necessarily within the deliverables, but still would prove useful to show the modifiability of the design when looking to integrate it within an actual aircraft. Since the main model, currently being iterated with a static test in mind, would not be designed for flight conditions- as it was not designed with these in mind- the thought arose that a second model could be adjusted from the first to include higher entrance speeds. CFD was used with higher speeds to create an inlet more viable for these conditions.

Solidworks flow simulation was used to conduct CFD tests on the preliminary inlet designs. For the CFD analysis, certain boundary conditions and goals need to be defined. The first boundary condition was placed at the inlet capture area. This boundary condition is an environmental pressure of 14.696 psi, which is the pressure at standard sea level conditions. The second boundary condition is an outlet mass flow placed at the exit of the inlet leading into the engine compressor. The engine pulls in air at a rate of 0.5512 pound mass per second, this is the outlet mass flow boundary condition for the inlet. To find the average total pressure drop through the inlet certain goals needed to be defined to calculate the difference in pressure. The first goal was an average total pressure goal at the inlet face, the second and third goals were total pressure goals at the two kiel probes at the entrance of the bell mouth transition duct, and the final goal was an equation goal to calculate the difference between the inlet total pressure and an average of the total pressures at the kiel probes. A depiction of the atmospheric conditions and the mass flow rate at the transition duct is shown in Fig. 5.

Global mesh settings were set to level 7, the finest possible. This was done to help gather data from the modeled probe faces and to allow calculation for pressure recovery percentages. For the analysis settings, it was set to internal flow with adiabatic conditions. The working fluid is air, and the flow type is both laminar and turbulent, with a wall roughness 36.96 microinches to match the roughness of printed filament. The finish settings had a refinement level of 5 for CFD tests. The analysis was set to complete once all predetermined goals were satisfied.

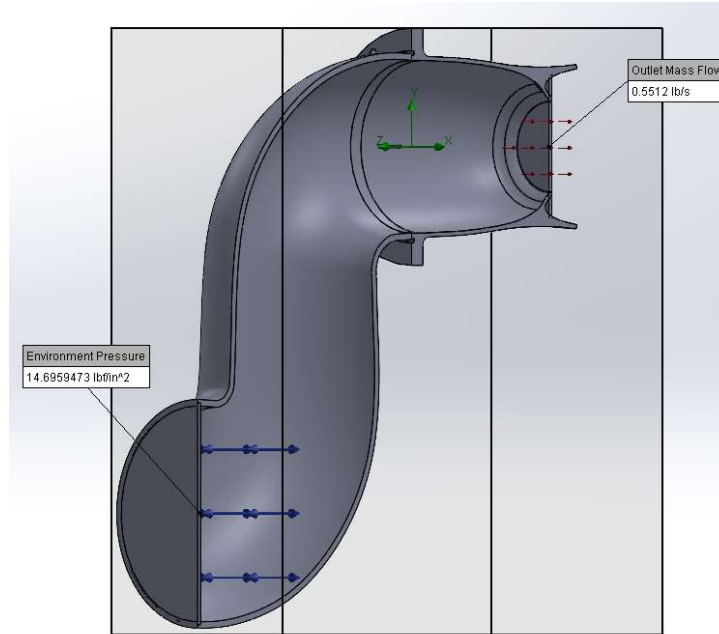


Figure 5: CFD Process Model

E. Finite Element Analysis

Before anything was mounted and constructed, FEA was undertaken to judge the safety of the plates mounting the engine to the thrust stand as well as FEA for the screws connecting the engine to the transition duct. Both were determined to be sufficiently safe for all foreseeable forces. All presented results from the team's analyses for the mounting plates, engine mounting ring, and the screws mounting the transition duct with a high estimate beyond what is expected.

The JetCat P100-RX model, shown in Fig. 6, was used for the FEA. The transition duct attachment screws, placed equidistant from one another, is shown in Figure 7. FEA was conducted on the cowling screws that fasten in the transition duct as well as secure the inlet weight to the engine. In the most extreme case, which would entail some external force on the inlet causing such a force on the screws, fifteen pounds of force were distributed uniformly across the screws to simulate the downward resulting forces of the inlet and attachments on the screws, fixed into place by the engine. Even in this extreme case, the screws remained safe, over 1.0, and most of the body of the screw exceeded 1.6 as its factor of safety. For this case, the max stress felt in the body was also well below, around 60%, of the yield stress. FEA confirmed the preconceived ideas that the inlet would be safe and perform well, but it also gave the team a sense of confidence that future designs would be able to be supported so long as they were within any reasonable build.

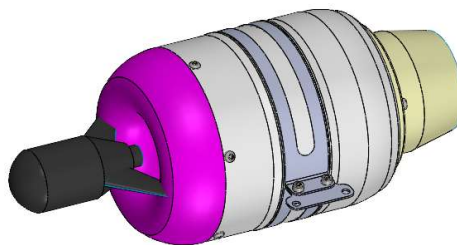


Figure 6: CAD Model of the JetCat P100-RX



Figure 7: CAD Model of Cowling with Screw Placement

Table 1: Finite Element Analysis Results

Force Applied	15 lbf
Maximum Von Mises Stress	24656 psi
Yield Strength	41046 psi
Maximum Displacement	4.45e-5 in
Minimum Factor of Safety	1.23

With the fifteen pounds of force modeled through FEA, which is far more than the teams reasonably expect, there was not enough stress to yield the material, the displacement was a fraction of a millimeter, and the factor of safety was over one. With these being stated, the teams were confident in their models not causing damage to the engine, the cowling screws, or the test stand in case of critical failure. Less force than modeled is expected to be attributed to the inlets, and the moment arm apparatus is expected to carry some force, but the inlets would not cause failure even if this were not the case. The FEA provided confidence in the teams' ability to move forward.

F. Passive Flow Control

Separation was seen as a big risk to the quality of the flow coming into the engine. There are two main ways to help this problem. The first is a longer, more gradual curve. Since length is a secondary criteria, this was seen as a less than ideal solution. The next mitigation plan was to potentially implement passive flow control. Passive flow control is described to be structures that are built into the design to help guide the flow. The idea for implementation of this concept is keeping the inside skin of this inlet rougher in this area. Since most of the inside was sanded to ensure the flow would be going over a smoother surface, leaving this area rougher than other places may have a greater effect on the flow. This may allow for the flow to be tripped and stay attached longer, much like the effect of dimples on a golf ball. However, the problem with this plan was the difficulty of implementation in a testing sense. Although the surface can be left rough, barring printing another inlet to completely smooth there was no way to truly test the effects of this roughness on the system. Although a good idea, the implementation means that an inlet will be completely wasted due to a tiny increase in performance over the other, differently sanded model.

An idea for more passive flow control is structures built into the design before printing. Structures, like dimples, could be built into the design. These however, were not seen as feasible for the scope of this project and further investigation was abandoned.

G. Non-Engineering Considerations

In addition to the foundation of engineering topics driving the design there were several other factors that affected the design. The ideal design concept was to be as non-complex as possible and this was intended to be resolved by using standard fastener sizes and simple assembly methods. The decision to use PLA to 3D print the inlets was to increase maintainability and allow for quick and inexpensive fabrication: usually around two days for and approximately \$20-\$30 per inlet, including epoxy. Overall quality of the design would be maximized by utilizing the PEEK filament for the final inlet fabrication which would offer much higher strength, durability, and temperature resistance as compared to PLA. The design must be designed to look aesthetically appealing. An ideal design would fit well with all components and be assembled in as few pieces as possible. This would reduce the number of sections to be epoxied and sanded which would help to make the inlet look more like one continuous piece once it is sanded and painted.

IV. Experimental Arrangement

The top view of the experimental setup shown in Fig. 8 displays the main structures associated with the current experiment plan. The engine as seen below is suspended within a circular mount attached to two mounting plates. Figure 8 shows the assembly fabricated to attach the transition duct to the inlet while relieving stress to the engine's cowling screws. This design is supported by the moment arm itself and not the surrounding safety cage or the table. No thrust loss will be expected from the arrangement due to the engine being rigidly attached to non-sensing elements. The plate conjoining the inlet and bell mouth transition piece was fabricated using wood as this material was cheap, strong enough to support the inlet, and easy to work with for the project.

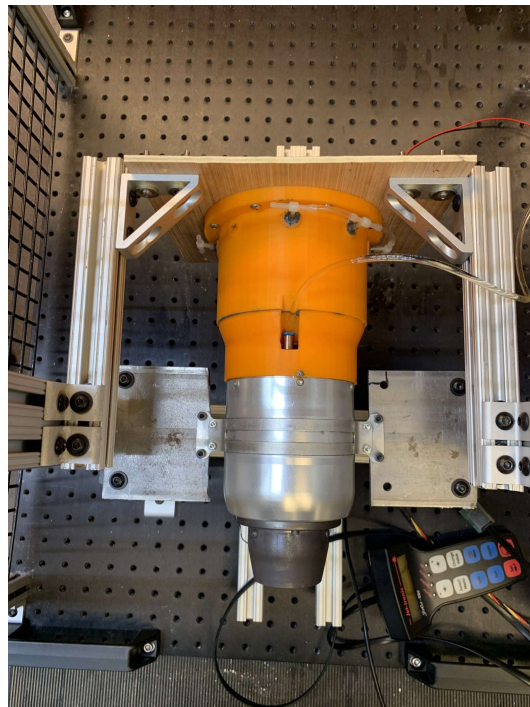


Figure 8: Top View of the Experimental Arrangement

Figure 9 illustrates an aft view of the test setup, this further visualizes how the supporting structure for the inlet and transition duct is assembled. The faint red wire in the background of the picture is the lead for the load cell that measures thrust. The black, yellow, and red wire bundle is the control harness for the engine and finally the clear line is a fuel line feeding fuel mixed with turbine oil to the engine.

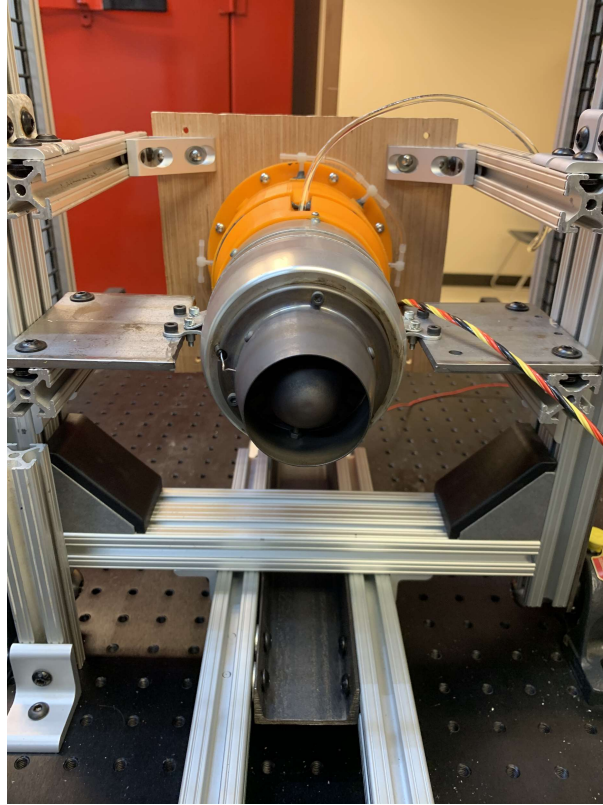


Figure 9: Back View of the Experimental Arrangement

Figure 10 is a profile picture of the test cell. Immediately aft of the wooden support plate are black spots with white and clear plastic tubing attached to them. These are static pressure ports, when coupled with a transducer these will measure static pressure while Kiel probes will be inserted at the 12 and 6 o'clock positions to measure total pressures. Having both static and total pressure measurements will allow the teams to characterize inlet performance in terms of pressure recovery and predict performance in AFRL's test cell.

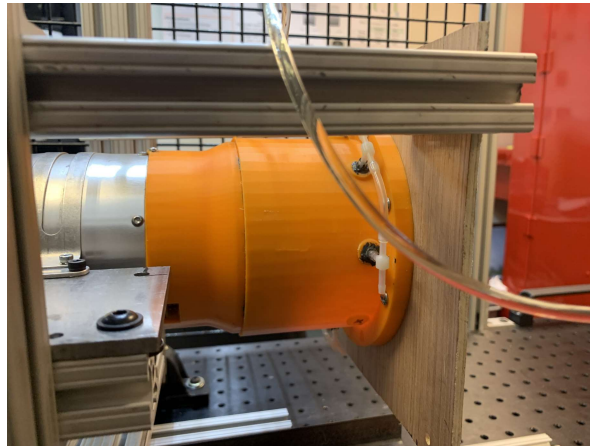


Figure 10: Side View of the Experimental Arrangement

Figure 11 is a front view of the test setup. This picture further details the inlet supporting structure. A black cylinder can be seen within the orange transition duct, this is the starter for the engine that the transition duct fits around. The transition duct is designed to replace the stock cowling of the engine while utilizing the stock cowling mounting screws. The silver circular pattern of screws is used to bolt the inlet to the support structure with the inlet

having an identical flange and bolt pattern. When tightened the soft wood will act as a seal providing, ideally, and airtight seal. If needed this sealing can be augmented using solid or liquid gasket material.

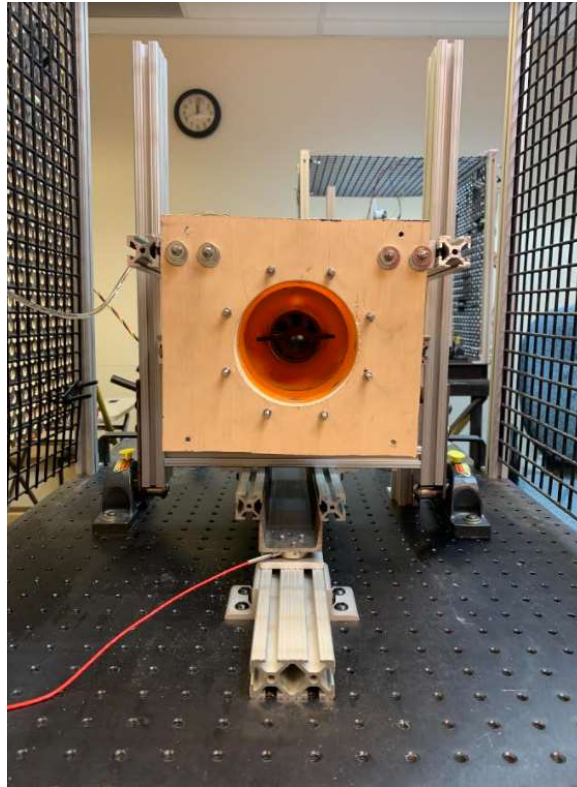


Figure 11: Front View of Experimental Arrangement Sans Inlet Design

The schematic for the engine test assembly can be seen below in Fig. 12. This schematic details all of the major components used to operate and control the Jetcat P100-RX and the connections that are used in order to acquire the engine performance data such as RPM and TSFC. Additionally, the schematic for the pressure data acquisition assembly can be seen in Fig. 13. In the assembly, two KAA-12 kiel probes are joined together through plastic tubing in order to find the average total pressure. This is then connected to a PX-409 absolute pressure R supplied by Omega. The static pressure ring is also connected to a PX-409 transducer. By knowing the static and total pressure, the dynamic pressure can then be found which indicates the velocity of the flow that is entering the engine. As it can be seen, these absolute pressure transducers convert the pressure inputs into a digital signal which is then directly imputed to a laptop. Through the use of the provided software, the pressure readings are then outputted.

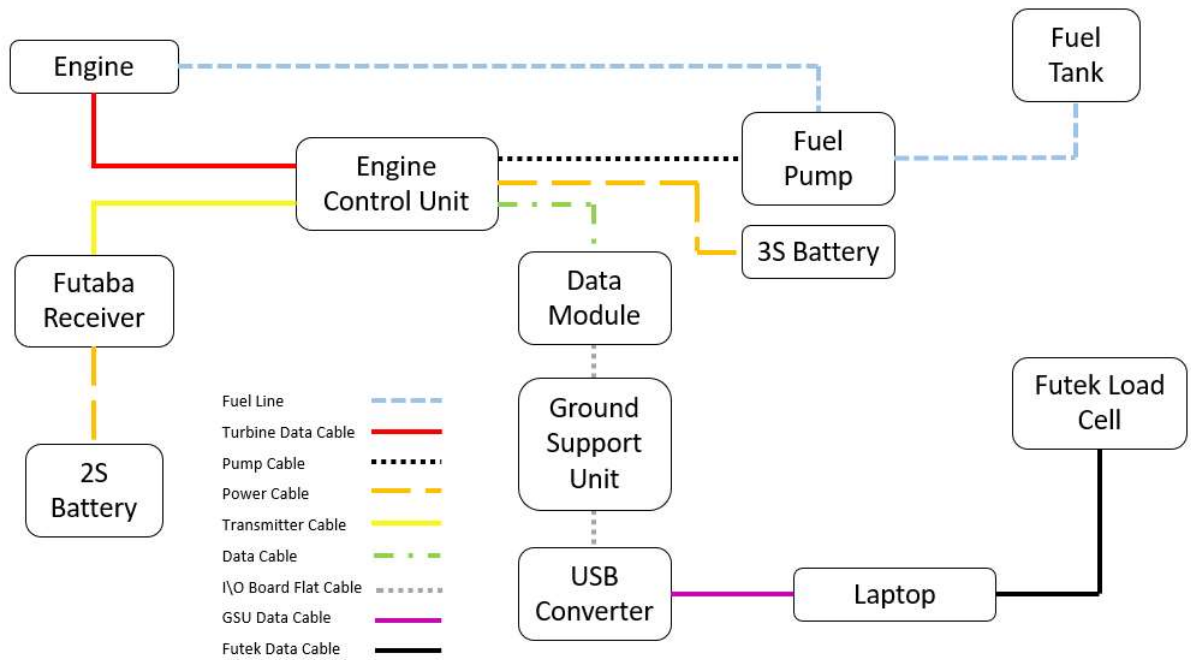


Figure 12. Engine Test Equipment Diagram

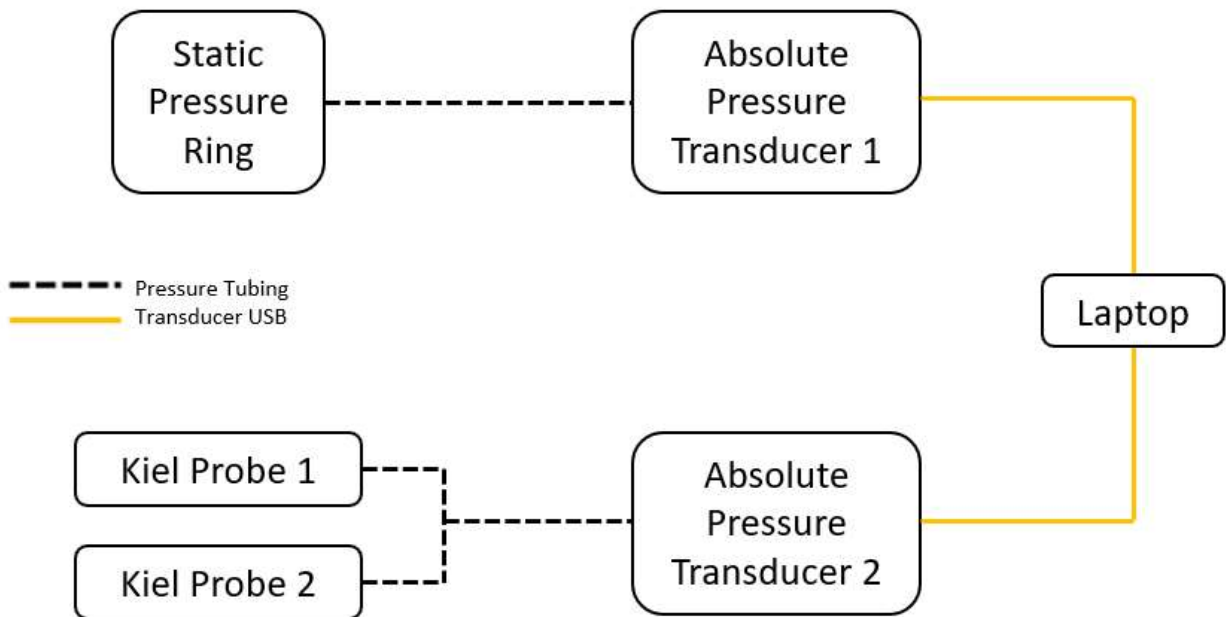


Figure 13. Engine Test Pressure Equipment Diagram

V. Analytical Design Process

A. Design Downselection and Analytical Results

The initial design selection was performed by narrowing down the geometry of the inlets by building a design matrix composed of inlet geometries and the important testing parameters. This design matrix can be seen in Table 3, and the test code legend can be seen in Fig. 14. Through this exercise, it was determined that there are three variables that drive the inlet design process. These are axial length, capture area, and inlet geometry. With the design matrix created, CFD was used to find general trends between the design variables in order to pick an initial design that would serve as a starting point.

Table 3. Inlet Concepts to Test

Code #	Shape	Capture Area (in ²)	Axial Length (in)	Angle (°)	Volume (in ³)
1.21	Circle	12.566	27.064	12.5	453.6
1.24	Circle	12.566	16.48	20	303.8
1.41	Circle	28.274	27.064	12.5	457.5
1.44	Circle	28.274	16.48	20	468.3
2.21	Elliptical	12.566	27.064	12.5	463.9
2.24	Elliptical	12.566	16.48	20	307.7
2.41	Elliptical	28.274	27.064	12.5	690.8
2.44	Elliptical	28.274	16.48	20	464.5
3.21	Rectangular	12.566	27.064	12.5	454.6
3.24	Rectangular	12.566	16.48	20	301.7
4.21	Asymmetrical	12.566	27.064	12.5	443.3
4.24	Asymmetrical	12.566	16.48	20	294.5

Test Code Legend

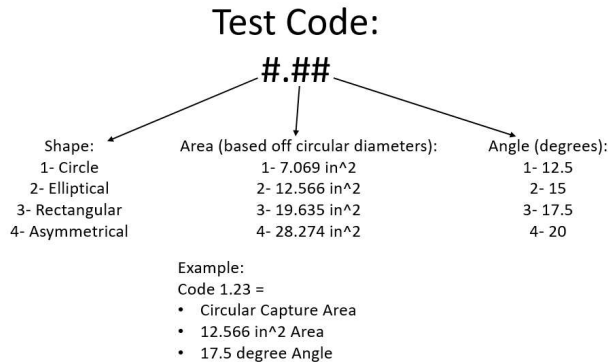


Figure 14. Inlet Test Code Legend

After the optimum design from the initial design matrix is chosen and the results from the CFD are verified, the axial length, inlet capture area, and the inlet geometry will be optimized to the design objectives. Once these three variables are optimized, passive flow control techniques will be explored in order to try and further decrease the pressure drop before the AFRL demonstration.

i. CFD Analysis

To understand the behavior of pressure loss for varying shape, area, and axial lengths of the concept inlets, CFD analysis was conducted for each preliminary inlet design. The CFD tests were performed with the boundary conditions and goals as stated in Section II part C. After CFD for each inlet was performed, the results were